Mechanisms of improving the mechanical and antibacterial properties of Ti-3wt.%Cu alloys

Chenxu Ma[1], Mengzhen Zhu[1], Jianying Wang[1], Xiongwen Zhou[2], Haixia Xing[3], Shouxun Ji[4], Hailin Yang[1]*

1. State Key Laboratory of Powder Metallurgy, Central South University, Changsha 410083, China

2. Department of Prosthodontics, Centre of Stomatology, Xiangya Hospital, Central South University, Changsha, 410008, China

3. Department of General Dentistry, Peking University School and Hospital of Stomatology, Beijing, 100081, China

4. BCAST, Brunel University London, Uxbridge, Middlesex UB8 3PH, United Kingdom

* Corresponding author: Tel.: +86-0731-88876644; E-mail: y-hailin@csu.edu.cn

Abstract: The mechanisms for the significantly improved mechanical properties and antibacterial rate against *Staphylococcus aureus* were studied in Ti-3wt.%Cu alloys obtained by spark plasma sintering (SPS) with subsequent cold rolling, and annealing. The tensile strength and elongation were 683.43 MPa and 21.55% respectively, while the antibacterial rate was 95% in the experimental alloys. The improvement can be attributed to the high efficiency generated by high-density *in-situ* Ti_2Cu precipitates in the refined grain structures of the experimental Ti-Cu alloys.

Keywords: Biomaterials; Microstructure; Powder technology; Nanoparticles

1. Introduction

Copper is used in many fields due to its excellent thermal and electrical properties, but the application as biomaterials is still under development for antibacterial properties [1,2]. Currently, Ti-Cu alloys have attracted great interest in the applications in dental and orthopaedic implants [3]. Previous studies have indicated that the antibacterial rate of Ti-Cu alloys fabricated by casting and powder metallurgy (P/M) methods was closely related to Cu contents, and the higher Cu content delivered better antibacterial properties [4,5]. Regrettably, excessive Cu addition would impair plasticity generate cytotoxicity, nausea and diarrhoea [6]. For instance, Aoki et al. [7] reported that the elongation of Ti-Cu alloy was only 1% when the copper content was 10 wt.%. Therefore, the balance between mechanical and antibacterial properties is essential for alloy and technical development. Particularly, the improved antibacterial properties in the alloys with less Cu contents are critical, but limited achievements have been reported in the literature.

In this work, we explore the capability of improving the mechanical properties and antibacterial rate of Ti-Cu alloys processed by SPS with subsequent plastic deformation of rolling and annealing. The improvement mechanism was focused on the relationship between the microstructure and mechanical and antibacterial properties. We aim to provide a technical approach to improve the mechanical and antimicrobial properties in Ti-Cu alloys through optimal rolling and heat treatment after SPS processing.

2. Experimental

The chemical compositions of the powder analyzed by inductively coupled plasma spectrometry (ICP-AES) was listed in Table 1. The Ti-3wt.%Cu pre-alloyed powder was consolidated through an SPS furnace (FCT SPS Systems GmbH) at 1150 ºC with a vacuum level of $<1\times10^{-2}$ Pa, and holding for 15 min at 40 MPa to form a product named as Ti-3Cu (S). Then, Ti-3Cu (S) was cold rolled using a mill (K101) for 10 times to reach the reduction of thickness by 40%, named Ti-3Cu (CR). Finally, the Ti-3Cu (CR) was annealed at 700ºC for 1 h and subsequently cooled to room temperature in the furnace named as Ti-3Cu (700). An electrical discharge machining was used to cut the tensile samples into a gauge length of 13 mm, cross-section of 4 × 2 mm^2 and antibacterial samples into Φ15 × 2 mm^3.

The microstructure was characterized using scanning electron microscopy (FEI nano 230 field emission, SEM), electron backscattered diffraction (EBSD) and transmission electron microscopy (TEM). Tensile tests were performed using a MTS Alliance RT30 tension machine with a crossed rate of 0.5 mm/min. The antibacterial test was performed according to the China Standard GB/T 2591 (equal to JIS Z 2801-2000) [3]. Using the following formula to calculate the antibacterial rate of the samples: $R_{(Antibacterialrate)}=(N_{control}-N_{test})/N_{control}\times 100\%$, where $N_{control}$ is the number of bacterial colonies on the control sample (cp-Ti), and N_{test} is the number of colonies of Ti-3Cu alloys under different conditions.

3. Results and discussion

Fig. 1 shows the microstructure of Ti-3Cu (S) and Ti-3Cu (700) alloys. The Ti-3Cu (S) was mainly composed of white phases with a laminar morphology (α-Ti + eutectoid Ti_2Cu) and light grey phases (α-Ti), which is consistent with the previous results [6]. After rolling and annealing, the Ti_2Cu phase changed from laminar to spherical shapes, and some Ti_2Cu phases were precipitated from the α-Ti matrix. Figs. 1b and 1d show the EBSD maps of the Ti-3Cu (S) and Ti-3Cu (700) alloys, respectively. Ti-3Cu (S) showed a typical lath-shaped structure of α-Ti. Numerous uniformly oriented grains in the microstructure resulted from nucleation from the same β-Ti grain boundary or grain interior. Compared with Ti-3Cu (S), Ti-3Cu (700) alloy showed significantly refined grain structures with different degrees of recrystallization.

Fig. 2 presents the TEM images of Ti–3Cu alloys under different conditions. Similar to the SEM result, a typical band eutectoid phase with 800 nm in width, was observed in Ti-3Cu (S) alloy (Figs. 2a and 2b). Two differences were found in the microstructure of Ti-3Cu (700) alloy: (*i*) the much narrower band eutectoid phase (685 nm) than that in the Ti-3Cu (S) alloy (Fig. 2c); (*ii*) a large number of spherical Ti_2Cu phases precipitated from the α-Ti matrix (the SAED pattern L1 inserted in Fig. 2d), and the eutectoid Ti_2Cu phases occurred spheroidize. Qualitative chemical analysis of the Ti_2Cu phases was also performed using HADDF. The corresponding results for different constituent elements are shown in Figs. 2g-i. Obviously, the *in-situ* phase was enriched in Ti and Cu elements.

The mechanical properties of the Ti-3Cu alloys are shown in Fig. 3a. It is seen that the subsequent rolling and annealing significantly increased the yield strength and UTS of Ti-3Cu (S) alloy, achieving 553.98 and 683.43 MPa, respectively, while maintaining good fracture strain of 21.55%. Compared with the materials made by casting [3,4,6], the Ti-3Cu (700) alloy delivered superior comprehensive mechanical properties. The strengthening mechanisms rationalize the enhancement in the strength of Ti-3Cu alloys. Rapid cooling during SPS has a high solute solubility of Cu and Ti_2Cu in the α-Ti matrix, increasing solid solution strengthening. Admittedly, the solid solution effect introduced by the high content Cu weakens due to the formation of in-situ Ti_2Cu after annealing. Moreover, the band eutectoid *in-situ* Ti_2Cu precipitates and Ti_2Cu phase act as a hard phase to hinder the movement of dislocations. Moreover, the interaction between Ti_2Cu particles with dislocation can be observed in Fig. 2f. Regrettably, the effect of Orowan strengthening would not be effective due to the relatively large size of particles. Furthermore, according to the classical strengthening theory, the resistance of the dislocation movement is calculated as follows: [8]

$$\tau = Gb/l \qquad (1)$$

where τ is the stress of the dislocation movement, G is the shear modulus, b is the Berger dislocation vector of the dislocation, and l is the particle's distance. The reduced distance of the eutectoid structure brings a higher resistance to dislocation movement. Also, the refined matrix in induced by the rolling brings a high strength induced by grain boundary strengthening.

Figs. 3c-e indicates a typical *S.aureus* colony cultured on Ti-3Cu alloys for 24 hrs and calculated antibacterial rate, and cp-Ti was used as a control group. The surface of cp-Ti is covered with bacterial colonies, while Ti-3Cu (S) alloy has only partial colonies, and Ti-3Cu (700) alloy has almost no colonies attached. Meanwhile, Fig. 3b shows the calculated antibacterial rate of Ti-3Cu (S) and Ti-3Cu (700) alloys. According to SN/T 2399-2010, antibacterial rate conforming to grade II (90% ≤ II < 99%) means that the material has antibacterial property. After rolling and annealing, the calculated antibacterial rate of Ti-3Cu alloy increased from 77% to 95%, showing excellent antibacterial property. Previous studies indicated that Ti_2Cu has a greater effect on antibacterial performance [3]. High volume fraction of Ti_2Cu phases can accelerate the release of Cu^{2+}, providing excellent antibacterial properties [6]. Meanwhile, compared with the Ti-3Cu (S), the Ti-3Cu (700) alloy (Fig. 2d) showed the size of Ti_2Cu phases about 200-500 nm, while the width of striped eutectoid phases is from ** to **. The size of *S. aureus* is about (500-800 nm) [10]. Therefore, the larger spherical Ti_2Cu phase in Ti-Cu alloy is more likely to effective contact *S. aureus* and thus inhibit the growth of bacteria adhering to the surface. Wang et al. [9] reported that the antibacterial mechanism of silver nanoparticles is the electron transfer between Ag nanoparticles and bacteria, and the size of Ag nanoparticles significantly affects the antibacterial effect of the material. Peng et al.[10] reported that Ti-Cu alloys with the larger spherical Ti_2Cu precipitate have an excellent antibacterial rate than laminar Ti_2Cu due to the larger contact area, which is similar to this study. The improved antibacterial performance is attributed to the increased volume fraction of the Ti_2Cu phase and large spherical Ti_2Cu.

4. Conclusions

In summary, cold rolling with subsequent annealing can significantly improve the mechanical and antibacterial properties of SPSed Ti-3Cu alloys, making it applicable for biomaterials. The *in-situ* Ti_2Cu phase plays a vital role in improving mechanical and antibacterial properties.

Declaration of Competing Interest

The authors declare that they have no known competing financial interests or personal relationships that could have influenced the work reported in this paper.

Acknowledgements

This work is financially supported by National Natural Science Foundation of China (Grant No. 51404302 and 51801003) and Natural Science Foundation of Hunan Province (Grant No. 2020JJ4732).

References

[1] W. Zhang, X. You, D. Fang, J. Tao, F. Yang, Influence of acid-treated time of carbon nanotubes on mechanical property in carbon nanotubes reinforced copper matrix composites, Diam. Relat. Mater. 109 (2020) 108069.

[2] W. Tong, D. Fang, C. Bao, F. Li, X. You, C. Li, J. Yi, Enhancing mechanical properties of copper matrix composite by adding SiO2 quantum dots reinforcement, Vacuum. 195 (2022) 110682.

[3] J. Wang, S. Zhang, L. Ren, K. Yang, Optimization of mechanical property, antibacterial property and corrosion resistance of Ti-Cu alloy for dental implant, J. Mater. Sci. Technol. 35 (2019) 2336–2344.

[4] M. Takahashi, M. Kikuchi, Y. Takada, O. Okuno, Mechanical Properties and Microstructures of Dental Cast Ti-Ag and Ti-Cu Alloys, Dent. Mater. J. 21 (2002) 270–280.

[5] E. Zhang, F. Li, M. Li, K. Yang, A new antibacterial titanium-copper sintered alloy: Preparation and antibacterial property, Mater. Sci. Eng. C. 33 (2013) 4280–4287.

[6] H.L. Yang, M.Z. Zhu, E.L. Zhang, S.X. Ji, Optimization of mechanical and antibacterial properties of Ti-3wt%Cu alloy through cold rolling and annealing, Rare Met. (2021).

[7] T. Aoki, I.C.I. Okafor, Y. Oda, T. Okabe, Mechanical properties of cast Ti-6Al-4V-XCu alloys, J. Oral Rehabil. 31 (2004) 1109–1114.

[8] X. Yao, Q.Y. Sun, L. Xiao, J. Sun, Effect of Ti2Cu precipitates on mechanical behavior of Ti-2.5Cu alloy subjected to different heat treatments, J. Alloys Compd. 484 (2009) 196–202.

[9] G. Wang, W. Jin, H. Feng, P.K. Chu, Antibacterial effects of titanium embedded with silver nanoparticles based on electron-transfer-induced reactive oxygen species, Biomaterials. 124 (2017) 25–34.

[10] C. Peng, S. Zhang, L. Ren, K. Yang, Effect of annealing temperature on mechanical and antibacterial properties of Cu-bearing titanium alloy and its preliminary study of antibacterial mechanism, Mater. Sci. Eng. C. 93 (2018) 495–504.

Figures and Tables

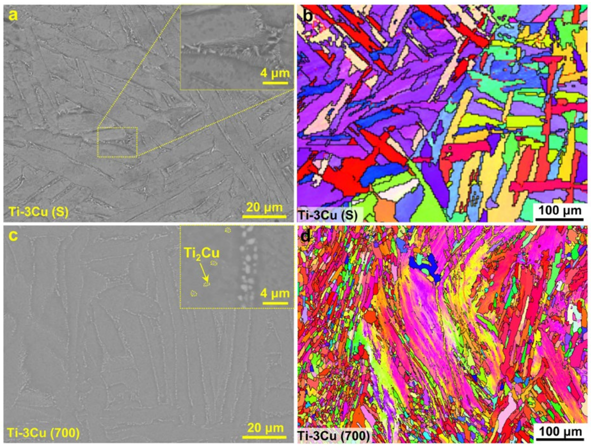

Fig. 1. SEM and EBSD micrographs showing the microstructure of Ti-3Cu (S) alloy (a & b), and (c & d) Ti-3Cu (700) alloy.

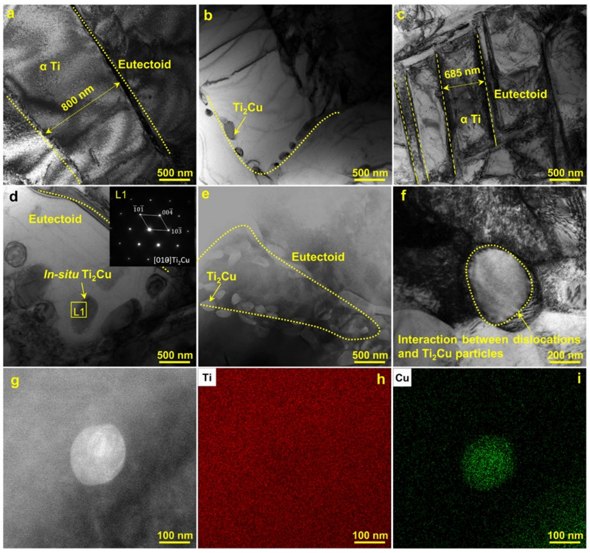

Fig. 2. TEM images of Ti-3Cu (S) alloy (a, b) and (c-f) Ti-3Cu (700) alloy; (a) distance between band eutectoid Ti_2Cu phases (800 nm); (b) Ti_2Cu particles distributed at the edge of eutectoid Ti_2Cu phases; (c) distance between band eutectoid Ti_2Cu phases; (d)

TEM with SAED (L1), and (e) STEM image showing *in-situ* Ti_2Cu particles distributed within eutectoid network; (f) the interaction between dislocations and Ti_2Cu particles; (g-i) the corresponding EDS mapping of Ti_2Cu particles.

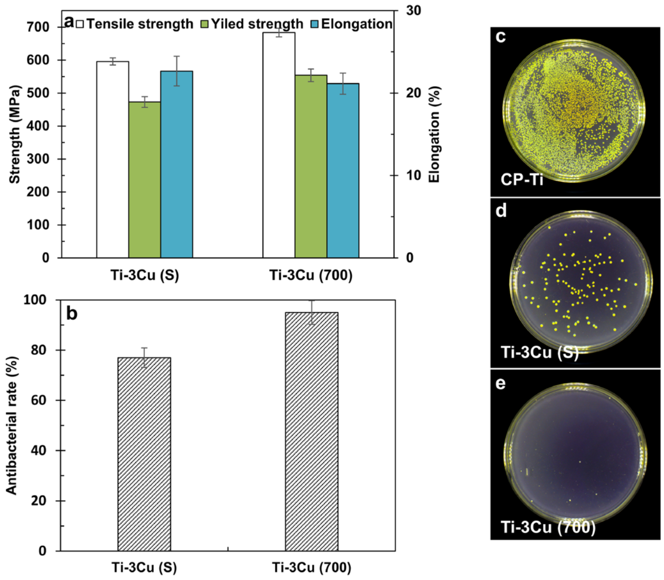

Fig. 3. (a) Mechanical properties of Ti-3Cu alloys under different conditions, (b) antibacterial rate of Ti-3Cu alloys against *S. aureus* under different conditions, and (c-e) *S. aureus* colonies after 24 hrs incubation on different Ti-3Cu alloys, (c) cp-Ti, (d) Ti-3Cu (S) alloy, and (e) Ti-3Cu (700) alloy.

Table 1. Chemical Compositions of experimental powder calibrated by ICP-AES (wt.%).

Element	N	C	H	O	Cu	Fe	Ti
wt.%	0.0011	0.036	0.0011	0.12	2.91	0.02	Bal.